Figure 3.1.6 SEM Micrograph of an Alumina Particle in a Spent Catalyst Mixture.

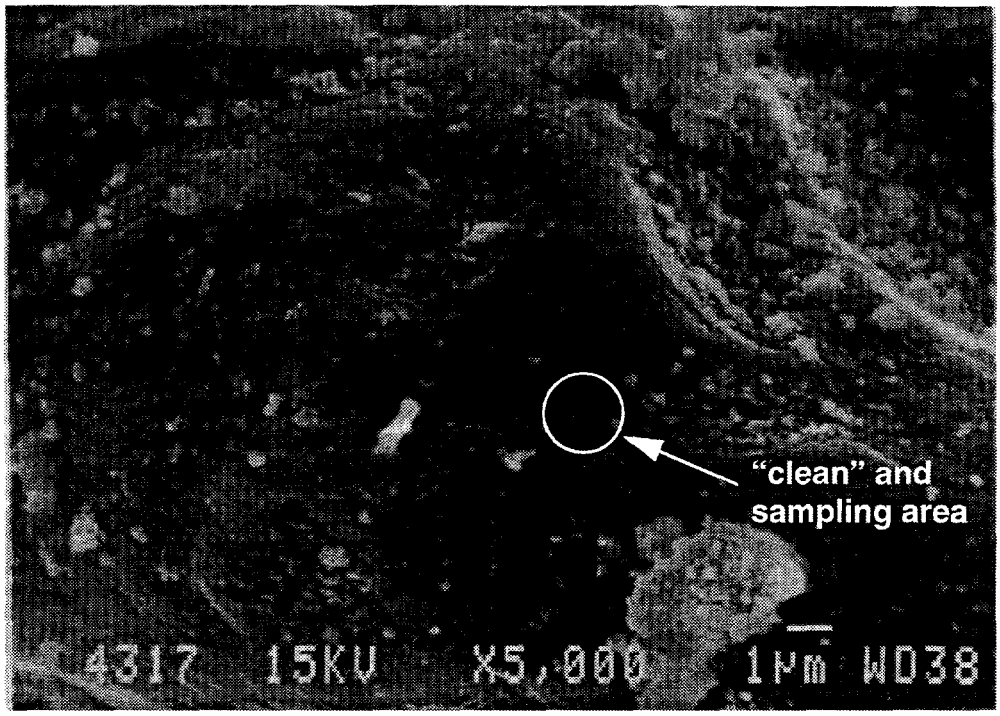

Figure 3.1.7 SEM Micrograph of an Alumina Particle in a Dispersed Spent Catalyst Mixture

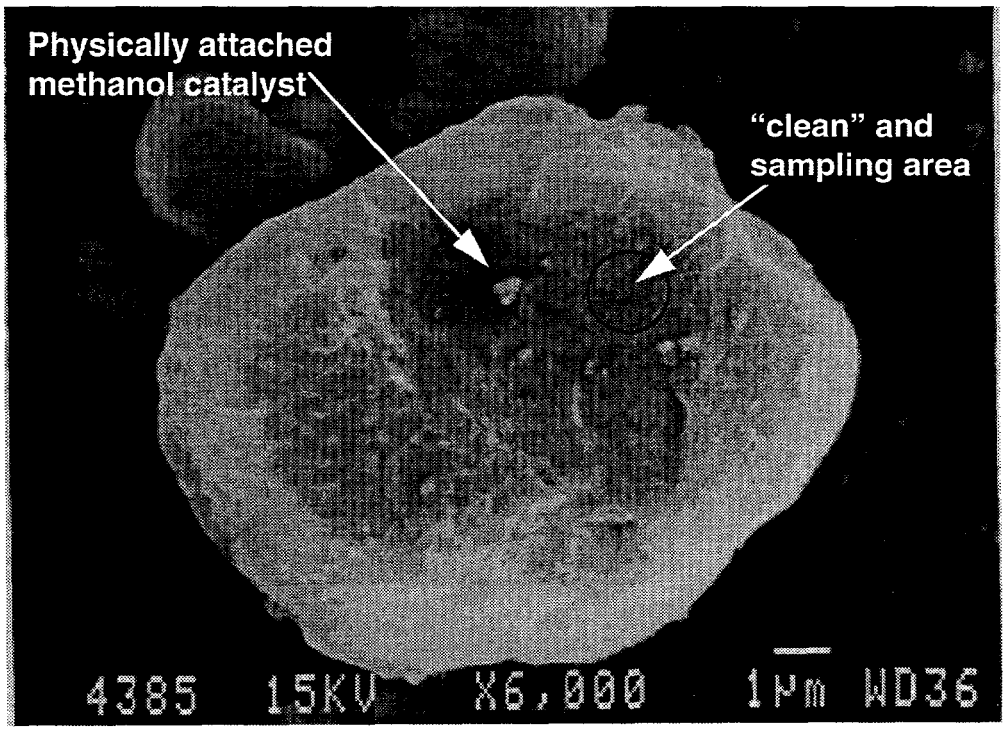

sem1.ppt

Figure 3.1.8 illustrates how a typical analysis was conducted. An SEM micrograph of an alumina particle, a cross section in this case, was generated first. Then the electron beam was *parked* at different spots in this cross section, and an EDS elemental analysis was performed. The sampling volume in this mode of analysis was an order of magnitude smaller than the dimension of alumina particles. Alternatively, one could *raster* the beam across the sample to obtain integrated elemental information.

Figure 3.1.8 SEM Micrograph of the Cross Section of an Alumina Particle in a Spent Catalyst Mixture

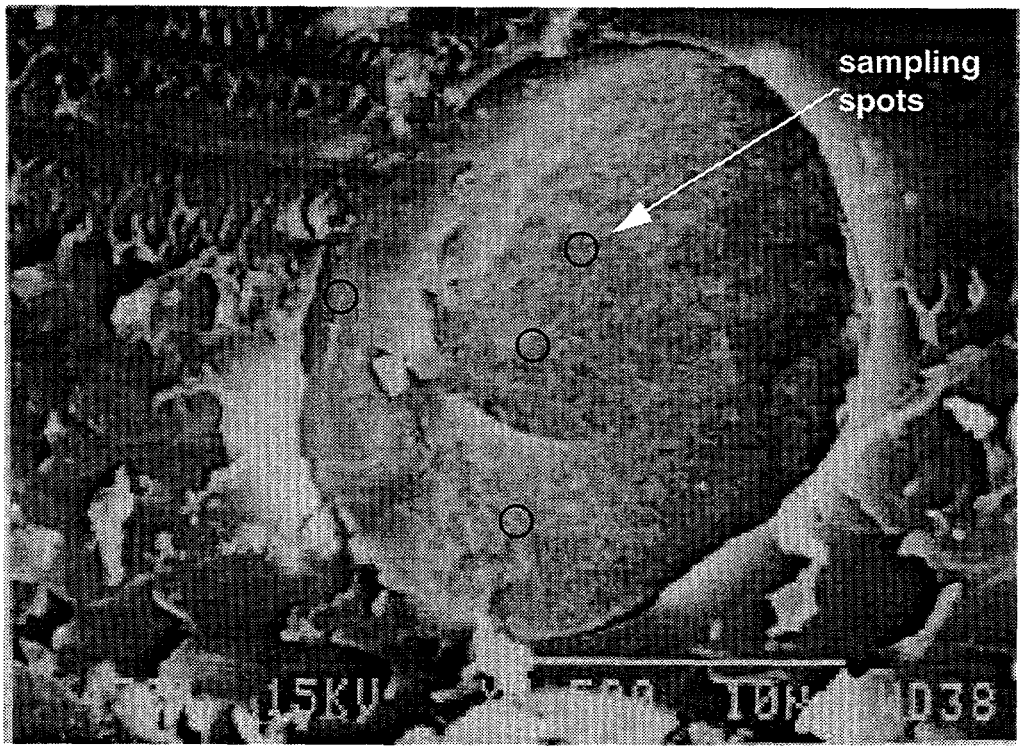

The elemental analysis by EDS is based on the energy dispersion of the X-ray generated by the same electron beam that is used for SEM. Figure 3.1.9a illustrates how different elements in a methanol catalyst sample appear on an EDS spectrum. (The aluminum section of the spectrum is not shown.) The net peak area was used for quantitative analysis. The integration was conducted using graphics software called Origin, since the data processing software used by the EDS instrument tended to draw erroneous baselines, especially when the signal was weak. To make sure the quantitation was independent of analytical conditions, such as the size of sample particles and the electron beam, gold coating, and parking mode vs. rastering mode, we looked at methanol catalyst particles of different sizes, with and without gold coating (gold coating was used to remove the static charging on the sample), and of different origins. The particles included those in a pure, freshly reduced methanol catalyst sample, in a spent catalyst mixture, and those physically attached to the outer surface of alumina particles in the same spent catalyst mixture. As shown by the solid dots in Figure 3.1.10, the Zn-to-Cu ratio from these different samples falls into a narrow range around 0.29, indicating that the quantitation is insensitive to the analytical conditions.

Figure 3.1.9 EDS Spectra of Different Samples

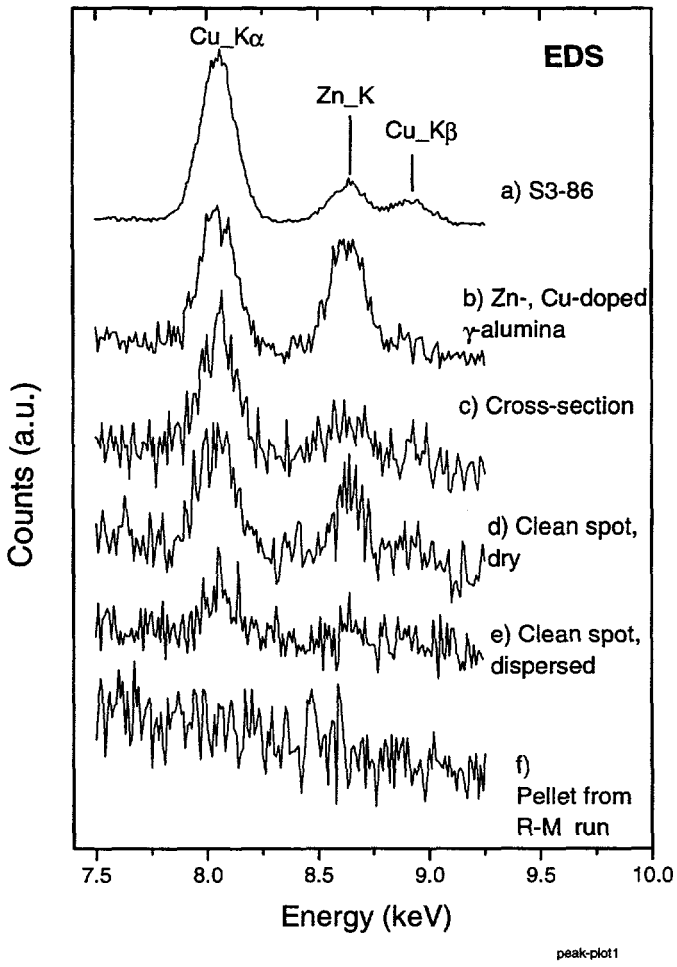

Figure 3.1.10 Zn-to-Cu EDS Peak Ratio of Different Samples

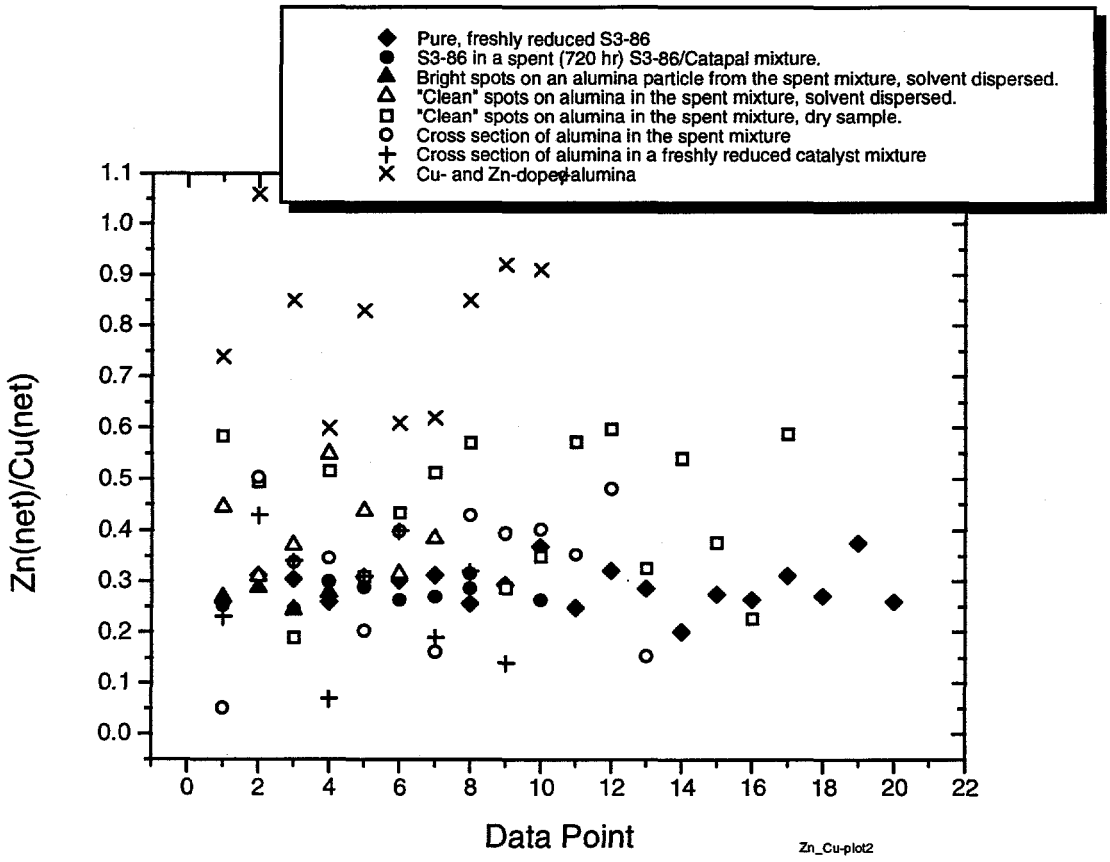

Since the absolute quantitation was difficult to measure, we relied on relative quantity of different elements for our analysis. These included ratios of (Zn+Cu) to Al and Zn to Cu. The (Zn+Cu) to Al ratio is intended as a measure of how much zinc and copper migrate onto the alumina, while the Zn to Cu ratio serves as a way to distinguish migrated zinc and copper from that in the physically attached methanol catalyst particles. We assume that zinc and copper deposition on the alumina due to the migration is unlikely to have the same ratio as in the methanol catalyst.

Results and Discussion

All EDS results, that is, the net peak area of Cu, Zn, and Al plus their ratios, are summarized in Table 3.1.1. Figure 3.1.9 displays typical EDS spectra from different samples. The Zn/Cu and (Zn+Cu)/Al ratios from different samples are shown in Figures 3.1.10 and 3.1.11. The three main samples discussed below are the alumina in a catalyst mixture that was on stream for 710 hours (*the spent sample*), the alumina in a freshly reduced catalyst mixture (*the freshly reduced sample*), and the alumina in a catalyst mixture used in a catalyst compatibility study (*the compatibility sample*). The relative activities of these three catalyst systems, in terms of the methanol equivalent productivity, are 0.6, 1, and 0.5, respectively. The analytical results from these samples do not show a consistent picture. The data that appear to support the migration theory will be examined first.

Table 3.1-1: Summary of EDS Analysis Results

Spectrum	Sampled particle	Region	Description	Beam mode	net Cu_Ka	net Zn_K	net Al_K	Zn_K/Cu_K	(Cu_K+Zn_K)/Al_K
1. Spent pure methanol catalyst. On syngas stream for 30 hr, 250 C, 750 psig, Texaco gas.									
J959001	S3-86	1	individual particle	parking	233.47	60.4	30.85	0.26	9.526
J959002	S3-86	2	individual particle	parking	237.18	73.79	32.28	0.31	9.634
J959003	S3-86	3	individual particle	parking	212.63	64.76	37.94	0.30	7.311
J959004	S3-86	4	individual particle	parking	267.22	69.29	31.19	0.26	10.789
J959005	S3-86	5	individual particle	parking	242.14	74.78	41.64	0.31	7.611
J959006	S3-86	6	individual particle	parking	226.88	68.51	35.06	0.30	8.425
J959007	S3-86	7	individual particle	parking	217.82	67.92	49.19	0.31	5.809
J959008	S3-86	8	individual particle	parking	262.87	67.34	26.11	0.26	12.647
J959009	S3-86	9	individual particle	parking	242.56	71.16	30.91	0.29	10.149
J959010	S3-86	10	individual particle	parking	189.82	69.96	109.24	0.37	2.378
J959011	S3-86	11	individual particle	parking	242.91	60.18	34.8	0.25	8.709
J959012	S3-86	12	individual particle	parking	216.56	69.57	115.05	0.32	2.487
J959013	S3-86	13	individual particle	parking	234.61	67.22	64.22	0.29	4.700
J959014	S3-86	14	individual particle	parking	276.92	55.79	25.38	0.20	13.109
J959015	S3-86	15	individual particle	parking	261.17	71.98	36.04	0.28	9.244
J959016	S3-86	16	individual particle	parking	262.23	69.14	33.92	0.26	9.769
J959017	S3-86	17	individual particle	parking	232.69	72.38	54.52	0.31	5.596
J959018	S3-86	18	individual particle	parking	269.95	73.31	15.98	0.27	21.481
J959019	S3-86	19	individual particle	parking	191.81	71.92	147.92	0.37	1.783
J959020	S3-86	20	individual particle	parking	254.24	66.16	65.68	0.26	4.878
2. Catalyst mixture on syngas stream for 710 hours (250 C, 750 psig, H2-rich gas).									
j950804	alumina	4	dry, clean spot	parking	3.82	2.23	1046.73	0.58	0.006
j950805	alumina	5	dry, clean spot	parking	4.21	2.08	1053.04	0.49	0.006
j950806	alumina	6	dry, clean spot	parking	4.47	0.85	1203.49	0.19	0.004
j950807	alumina	7	dry, clean spot	parking	4.78	2.47	1093.26	0.52	0.007
j950808	alumina	8	dry, clean spot	parking	5.68	1.76	972.25	0.31	0.008
j950809	alumina	9	dry, clean spot	parking	9.88	4.29	719.93	0.43	0.020

Table 3.1-1: Summary of EDS Analysis Results (cont.)

Spectrum	Sampled particle	Region	Description	Beam mode	net Cu_Ka	net Zn_K	net Al_K	Zn_K/Cu_K	(Cu_K+Zn_K)/Al_K
j950810	alumina	10	dry, clean spot	parking	7.01	3.6	1037.1	0.51	0.010
j950811	alumina	11	dry, clean spot	parking	9.77	5.58	972.61	0.57	0.016
j950812	alumina	12	dry, clean spot	parking	9.4	5.53	947.93	0.59	0.016
j950813	alumina	13	dry, clean spot	parking	4.75	2.72	983.44	0.57	0.008
j950814	alumina	14	dry, clean spot	parking	5.42	3.24	1029.06	0.60	0.008
j950815	alumina	15	dry, clean spot	parking	9.38	5.08	584.03	0.54	0.025
j950816	alumina	16	dry, clean spot	parking	5.54	2.09	1068.74	0.38	0.007
j950817	alumina	17	dry, clean spot	parking	7.1	1.61	1142.79	0.23	0.008
j950818	alumina	18	dry, clean spot	parking	8.62	2.81	1188.99	0.33	0.010
j950819	alumina	19	dry, clean spot	parking	9.35	2.69	1118.31	0.29	0.011
j950820	alumina	20	dry, clean spot	parking	13.71	4.79	839.51	0.35	0.022
d0801b	alumina	1	dispersed, clean spot	parking	1.64	0.73	682.36	0.45	0.003
d0802b	alumina	2	dispersed, clean spot	parking	n.d.	n.d.	960.9		
d0804b	alumina	4	dispersed, clean spot	parking	n.d.	n.d.	1084.2		
d0805b	alumina	5	dispersed, clean spot	parking	2.42	0.75	972.97	0.31	0.003
d0806b	alumina	6	dispersed, clean spot	parking	n.d.	n.d.	1043.1		
d0807b	alumina	7	dispersed, clean spot	parking	3.41	1.87	999.15	0.55	0.005
d0808b	alumina	8	dispersed, clean spot	parking	little	little	982		
d0809b	alumina	9	dispersed, clean spot	parking	3.67	1.38	880.64	0.38	0.006
d0810b	alumina	10	dispersed, clean spot	parking	little	little	996.7		
d0811b	alumina	11	dispersed, clean spot	parking	little	little	996.7		
d0812b	alumina	12	dispersed, clean spot	parking	little	little	996.7		
d0813b	alumina	13	dispersed, clean spot	parking	n.d.	n.d.	1727.9		
d0814b	alumina	14	dispersed, clean spot	parking	2.83	1.24	1721.33	0.44	0.002
d0815b	alumina	15	dispersed, clean spot?	parking	8.47	2.67	1467.21	0.32	0.008
d0816b	alumina	16	dispersed, clean spot	parking	1.38	0.53	1481.3	0.38	0.001
d0817b	alumina	17	dispersed, clean spot	parking	n.d.	n.d.	1417.5		

Table 3.1-1: Summary of EDS Analysis Results (cont.)

Spectrum	Sampled particle	Region	Description	Beam mode	net Cu_Ka	net Zn_K	net Al_K	Zn_K/Cu_K	(Cu_K+Zn_K)/Al_K
d0818b	alumina	18	dispersed, clean spot	parking	n.d.	n.d.	1152.5		
d0819b	alumina	19	dispersed, clean spot	parking	n.d.	n.d.	1000.1		
d0820b	alumina	20	dispersed, clean spot	parking	n.d.	n.d.	1329.1		
d0803b	alumina	3	dispersed, bright spot	parking	160.84	46.24	193	0.29	1.073
d0821b	alumina	21	dispersed, bright spot	parking	219.57	58.95	100.81	0.27	2.763
d0822b	alumina	22	dispersed, bright spot	parking	223.47	54.32	75.68	0.24	3.671
d0823b	alumina	23	dispersed, bright spot	parking	204.59	56.83	70.89	0.28	3.688
x0801b	alumina	1	cross section, near center	parking	10.03	0.52	1991.62	0.05	0.005
x0802b	alumina	2	cross section, near center	parking	6.12	2.07	1958.28	0.34	0.004
x0803b	alumina	3	cross section, near center	parking	6.35	2.2	1939.4	0.35	0.004
x0804b	alumina	4	cross section, inclusion	parking	7.22	1.47	2399.42	0.20	0.004
x0805b	alumina	5	cross section, within section	parking	4.74	2.39	2100.33	0.50	0.003
x0806b	alumina	6	cross section, near edge	parking	10.6	4.23	2254.42	0.40	0.007
x0807b	alumina	7	cross section, near center	parking	4.6	0.71	174.13	0.15	0.030
x0808b	alumina	8	cross section, within section	parking	3.2	0.52	1137.66	0.16	0.003
x0809b	alumina	9	cross section, near edge	parking	2.35	1.01	1209.88	0.43	0.003
x0810b	alumina	10	cross section, near center	parking	2.38	0.94	1282.14	0.39	0.003
x0811b	alumina	11	cross section, near edge	parking	9.32	3.75	826.58	0.40	0.016
x0812b	alumina	12	cross section, within section	parking	3.23	1.14	1123.36	0.35	0.004
x0813b	alumina	13	cross section, near center	parking	1.91	0.92	1031.17	0.48	0.003
xr0801	alumina	1	individual cross section	rastering	7.29	0.92	1806.7	0.13	0.005
xr0802	alumina	2	individual cross section	rastering	9.46	3.15	1127.2	0.33	0.011
xr0803	alumina	3	individual cross section	rastering	9.75	2.02	1771.6	0.21	0.007
xr08e	epoxy	4	epoxy	rastering	n.d.	little	little		

Table 3.1-1: Summary of EDS Analysis Results (cont.)

Spectrum	Sampled particle	Region	Description	Beam mode	net Cu_Ka	net Zn_K	net Al_K	Zn_K/Cu_K	(Cu_K+Zn_K)/Al_K
3. Freshly reduced catalyst mixture.									
x2101	alumina	1	cross section region1	parking	5.15	1.2	2241.3	0.23	0.003
x2102	alumina	2	cross section region 2	parking	2.54	1.09	1341.8	0.43	0.003
x2103	alumina	3	cross section region 3	parking	11	3.72	1380.7	0.34	0.011
x2104	alumina	4	cross section region4	parking	0.59	0.04	1322.9	0.07	0.001
x2105	alumina	5	cross section region5	parking	13.61	4.22	1394.9	0.31	0.013
x2106	alumina	6	cross section region 6	parking	7.67	3.09	1519	0.40	0.007
xr2101	alumina	1	individual cross section	rastering	6.355	1.23	1721.3	0.19	0.004
xr2102	alumina	2	individual cross section	rastering	39.05	12.47	1822.4	0.32	0.028
xr2103	alumina	3	individual cross section	rastering	8.58	1.18	1097	0.14	0.009
xr21e	epoxy	4	epoxy area	rastering	n.d.	n.d.	n.d.		
d2101	alumina	1	dispersed, clean spot	packing	n.d.	n.d.	1395.4		
d2102	alumina	2	dispersed, clean spot	packing	n.d.	n.d.	2134.4		
d2103	alumina	3	dispersed, clean spot	packing	n.d.	n.d.	1868.2		
d2104	alumina	4	dispersed, clean spot	packing	n.d.	n.d.	1493.9		
d2105	alumina	5	dispersed, clean spot	packing	n.d.	n.d.	1721.8		
4. Catalyst mixture used in the catalyst compatibility experiment. Under 2% H2 for 120 hr, 250 C, 750 psig.									
x2601	alumina	1	cross section region1	parking	9.33	3.55	1728.3	0.38	0.007
x2602	alumina	2	cross section region 2	parking	6.49	1.77	1819.2	0.27	0.005
x2603	alumina	3	cross section region 3	parking	6.64	1.77	1867.1	0.27	0.005
x2604	alumina	4	cross section region4	parking	4.37	1.03	1592.3	0.24	0.003
x2605	alumina	5	cross section region5	parking	7.71	1.82	783.8	0.24	0.012
x2606	alumina	6	cross section region 6	parking	3.49	1.11	1537.9	0.32	0.003

Table 3.1-1: Summary of EDS Analysis Results (cont.)

Spectrum	Sampled particle	Region	Description	Beam mode	net Cu_Ka	net Zn_K	net Al_K	Zn_K/Cu_K	(Cu_K+Zn_K)/Al_K
5. Alumina pellets used in the run with R-M basket internals. On stream 503 hr, 250 C 750 psig, Shell gas.									
p4301g	alumina	1	outer surface, grey particle	parking	little	little			
p4301w	alumina	1	outer surface, white particle	parking	little	little			
p4302g	alumina	2	outer surface, grey particle	parking	0	0			
p4302w	alumina	2	outer surface, white particle	parking	0	0			
p4303g	alumina	3	outer surface, grey particle	parking	0	0			
p4303w	alumina	3	outer surface, white particle	parking	0	0			
px4301g	alumina	1	cross section, grey particle	parking	0	0			
px4301w	alumina	1	cross section, white particle	parking	3.01	1.81	1315.6	0.60	0.004
px4302g	alumina	2	cross section, grey particle	parking	0	0			
px4302w	alumina	2	cross section, white particle	parking	0	0			
px4303g	alumina	3	cross section, grey particle	parking	0	0			
px4303w	alumina	3	cross section, white particle	parking	0	0			
px4304g	alumina	4	cross section, grey particle	parking	4.94	1.39	1019.6	0.28	0.006
px4304w	alumina	4	cross section, white particle	parking	0	0			
px4305g	alumina	5	cross section, grey particle	parking	0	0			
px4305w	alumina	5	cross section, white particle	parking	0	0			
px4306g	alumina	6	cross section, grey particle	parking	0	0			
px4306w	alumina	6	cross section, white particle	parking	0	0			
6. Cu and Zn-doped gama-alumina (3.95 wt% Cu, 4.55 wt% Zn)									
x3401		1	cross section	parking	9.94	7.37	646.29	0.74	0.027
x3402		2	cross section	parking	22.97	24.38	1395.28	1.06	0.034
x3403		3	cross section	parking	23.59	20.01	1140.02	0.85	0.038
x3404		4	cross section	parking	17.08	10.25	676.88	0.60	0.040
x3405		5	cross section	parking	9.65	8.02	451.21	0.83	0.039
x3406		6	cross section	parking	16.17	9.83	557.89	0.61	0.047

Table 3.1-1: Summary of EDS Analysis Results (cont.)

Spectrum	Sampled particle	Region	Description	Beam mode	net Cu_Ka	net Zn_K	net Al_K	Zn_K/Cu_K	(Cu_K+Zn_K)/Al_K
x3407		1	cross section	parking	11.22	7.01	421.39	0.62	0.043
x3408		2	cross section	parking	20.42	17.34	890.79	0.85	0.042
x3409		3	cross section	parking	30.73	28.18	1382.98	0.92	0.043
x3410		4	cross section	parking	29.14	26.44	1934.22	0.91	0.029

little: Barely above the noise level.
n.d.: Not detectable.

The spent sample is a catalyst mixture that was on stream for 710 hr in a LPDME™ run. The methanol equivalent productivity dropped by 39% at the end of the run. Both the cross section and the "clean" area on the outer surface of the alumina particles in this spent mixture were analyzed with EDS. Zinc and copper were detected from all spots on the cross section and on the "clean" area of the outer surface of alumina in a *dry* sample. On the "clean" area of the outer surface of alumina in a *dispersed* sample, zinc and copper were detected on more than half of the spots (Figure 3.1.9 and Table 3.1.1).

The method used to distinguish the zinc and copper by migration from that in the methanol catalyst fines is to examine the Zn-to-Cu ratio because it is very unlikely that zinc and copper from the migration will have the same stoichiometry as that in the methanol catalyst. The open dots in Figure 3.1.10 show the Zn-to-Cu ratio from the spent sample. The data are very scattered compared to those from the methanol catalyst. However, they are not scattered evenly around those from the methanol catalyst, but, instead most of the data points lie above. The number average is 0.38 compared to 0.29 from the methanol catalyst. This suggests that the Zn and Cu detected from the spent sample derive from the migration of zinc- and copper-containing species during the run.

Other information supporting the migration theory is obtained from the alumina pellets used in the LPDME™ employing Robinson-Mahoney basket internals and a mixture of catalyst pellets. The methanol catalyst did not deactivate after 508 hr on stream in that run. The outer surface and the cross section of the alumina pellets from the run were analyzed by EDS. As shown in Table 3.1.1, Zn and Cu were not detected in most spots (16 of 18) examined. A typical EDS spectrum from this sample is shown in Figure 3.1.9f. A traditional elemental analysis using chemical digestion and atomic absorption also showed no zinc and copper buildup on the alumina. This indicates indirectly that the deactivation is related to zinc and copper migration.

Other results were puzzling. According to the migration hypothesis, the catalyst deactivation should be proportional to the extent of zinc or/and copper migration. It follows that the zinc and copper content in the freshly reduced sample (with a relative activity of 1) should be much lower than that in the spent sample (with a relative activity of 0.6). Therefore, experiments were conducted to measure the zinc and copper contents of the freshly reduced sample and compare them to that in the spent sample.

The solid dots in Figure 3.1.11 show the (Zn+Cu)/Al ratio from the cross section and "clean" area of the spent sample. The data are very scattered, ranging from 0.001 to 0.03, with a number average of 0.008. The three data points collected by rastering the electron beam across the cross-section of three alumina particles do not show better consistency, ranging from 0.005 to 0.01 (Table 3.1.1). No concentration gradient across alumina particles can be detected (Table 3.1.1). To estimate the concentration of zinc and copper in the alumina, a calibration sample was prepared by impregnating γ-alumina with 4.55 wt % zinc and 3.95 wt % of copper. The EDS results from this sample are shown in Figures 3.1.9, 3.1.10 and 3.1.11. The (Zn+Cu)/Al ratios from this sample, as shown in Figure 3.1.11, are also scattered, ranging from 0.027 to 0.047 with a number average of 0.038. Based on this standard, the concentration of zinc plus copper in the spent sample ranges from 0.2 to 6.7 wt %, with an average of 1.8 wt %.

Figure 3.1.11 (Cu+Zn)-to-Al EDS Ratios of Different Samples

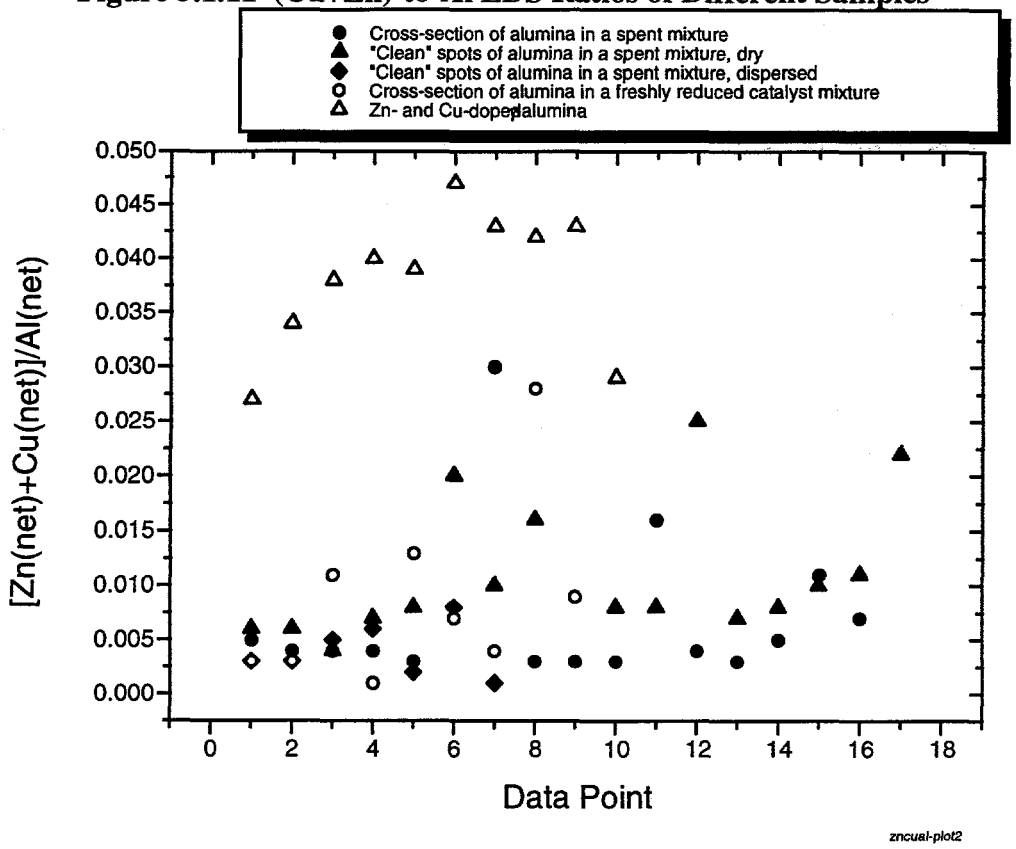

The open circles in Figure 3.1.11 are the (Zn+Cu)/Al ratios measured from the cross section of the freshly reduced sample. Zinc and copper were detected on all spots examined with EDS (Table 3.1.1). Again the data are scattered, but the range they cover is similar to that from the spent sample, with an average of 0.009. The zinc and copper contents in these two samples are similar to each other, although their activity is different by 40%. Further confusion comes from the Zn-to-Cu ratio measured from the freshly reduced sample. As shown in Figure 3.1.10, the data, with an average ratio of 0.27, are scattered around those from the methanol catalyst, with an average of 0.29, not above them as seen with the spent sample.

Also examined was the cross section of alumina particles in the catalyst mixture used in the catalyst compatibility experiment. In this experiment, the methanol catalyst and alumina were held together under 2% H_2 in N_2 and the reaction temperature (250°C) and pressure (750 psig) for 120 hours. The activity of the catalyst system, in terms of methanol productivity, dropped by 50%. Zinc and copper were detected from all spots examined on the cross section. As shown in Table 3.1.1, the average (Zn+Cu)/Al ratio from this sample is 0.006. This ratio is lower than that from the spent sample (0.008), although the spent catalyst system shows lower deactivation. The Zn-to-Cu ratio from the sample used in the compatibility study is 0.25 on average, again close to, but not greater than, that from the methanol catalyst (0.29).

It is certain from all of these analyses that zinc and copper are detected in the alumina particles in the catalyst mixture samples. However, it is not certain where they originate and how they are

It is certain from all of these analyses that zinc and copper are detected in the alumina particles in the catalyst mixture samples. However, it is not certain where they originate and how they are related to the catalyst deactivation. The detected zinc and copper in the cross sections could arise from several possible causes:

1) Migration from the methanol catalyst
2) Methanol catalyst fines smeared over the cross section by the cutting
3) Methanol catalyst fines that are small enough to enter the defects and even the pores (with a mean diameter of 60 angstroms) of the alumina particles.

The first possibility is the working hypothesis. The second possibility, that of smear-over, is very unlikely because little zinc and copper were detected on the epoxy around the alumina cross sections; therefore smear-over was ignored. The third possibility is important because if it occurs, adhering methanol catalyst particles will interfere with or may overshadow analysis of the presence of any copper and/or zinc that has migrated. Thus, when the Zn-to-Cu ratio is near that of the methanol catalyst, a definitive conclusion about migration cannot be made.

The best way to determine the third possibility is to examine the morphology of the zinc and copper inside the alumina particle (i.e., the cross section) using other techniques such as high resolution Transmission Electron Microscopy (TEM). This technique allows us to distinguish the presence of fines from atomically dispersed zinc and copper. The atomically dispersed zinc and copper arise most likely from the migrated species. If the methanol catalyst fines work their way into alumina particles, it would be impossible to verify the existence of migrated zinc and copper by elemental analysis. Nevertheless even if the third possibility were proven, it is strong evidence of intimate contact between the methanol catalyst and alumina which would allow the possibility of migration. Experiments have been designed to examine this issue using TEM.

The results discussed above demonstrate that catalyst deactivation is not correlated with (Zn+Cu)/Al ratio. Note, however, that if the zinc and copper detected derive partially or mainly from the methanol catalyst fines in the alumina, we would not expect such a correlation. *If the presence of copper and zinc arises only from the migration,* there could be two explanations for the lack of correlation. First, the migration may be responsible only for the initial deactivation of the catalyst system. It has been shown that deactivation during reduction contributes substantially to the initial catalyst deactivation. Therefore, once a catalyst mixture passes through the reduction stage, the zinc and copper level in the alumina will be similar. Second, the migration did occur, but it does not account for the deactivation of both catalysts. In other words, the migration hypothesis is not correct.

Finally, the quality of the EDS data was examined. As shown in Figures 3.1.10 and 3.1.11, both Zn/Cu and (Zn+Cu)/Al ratios from the alumina samples are very scattered. Is this due to the inhomogeneous nature of the samples, or to the noise level of the EDS spectra (see Fig. 3.1.9a-e)? The inhomogeneous nature of the samples may be the more likely reason. Figures 3.1.10 and 3.1.11 show that similar scattering is observed from the Zn- and Cu-doped alumina sample, while the signal-to-noise ratio in its EDS spectrum is satisfactorily low (Fig. 3.1.9).

Then one can question if our small amount of data are statistically sound, especially for the freshly reduced and the compatibility samples.

Task 3.2 New Fuels from Dimethyl Ether (DME)

Overall 4 QFY95 Objectives

The following set of objectives appeared in Section III of the previous Quarterly Technical Progress Report No. 3:

- Continue to screen immobilized catalyst candidates for hydrocarbonylation of dimethyl ether to ethylidene diacetate.

- Continue catalyst development work on the cracking of ethylidene diacetate to vinyl acetate and acetic acid.

Chemistry and Catalyst Development

(i) Dimethyl Ether to Ethylidene Diacetate (EDA)

The effort has focused on understanding the rhodium complexes anchored to the Reillex polymers for the catalytic conversion of DME to EDA.

Results and Discussion for Ionic Bound Catalyst

It was reported previously that problems were experienced in reproducing the data from our homogeneous catalytic runs when a 100 cc reactor instead of a 300 cc reactor was used. Therefore, it was decided to resume using the 300 cc reactor for further studies. The first reactions attempted were the homogeneous catalytic runs using $RhCl_3$. $3H_2O$ as the catalyst. The reaction conditions were as follows: $RhCl_3$. $3H_2O$(0.2g), CH_3COOH(145g), MeI(9.5g), DME(10.3g), CO/H_2(1:1), 1500 psi, 190°C. The overall time of reaction was 150 min, and samples were taken at 15, 30, 60, 90, 120, and 150 min for analysis by gas chromatography. The reactions were performed three separate times, and the data obtained were found to be reproducible. As reported in earlier experiments, the mass balances were found to progressively worsen with time. A typical reaction profile is shown below in Figure 3.2.1. The highest yield of EDA based on DME added was ~17% at the 90 minute mark. Earlier work published in a European patent showed a much higher yield (at least 3 times greater) of EDA. Also, the results were obtained over shorter periods (45 & 90 min), and no samples were taken during the course of the reaction. It was decided to repeat the catalytic run in a batch mode for 60 min and analyze the products at the end of the reaction. The reaction profile for this one point is shown below in Figure 3.2.2.

The yield of EDA obtained in this reaction was much higher (44%), and a comparison of the reaction profile shown in Figure 3.2.2 with the sampling mode at the 60 min mark (see Figure 3.2.1) shows interesting differences. In the batch mode the EDA concentration is higher than the acetic anhydride concentration or the acetaldehyde concentration, whereas in the sampling mode, the concentration profile is totally reversed. Based on these results it was decided to conduct heterogeneous catalysis runs in a batch mode and compare them to a sampling mode.

Figure 3.2.1 Reaction Profile Sampling Mode

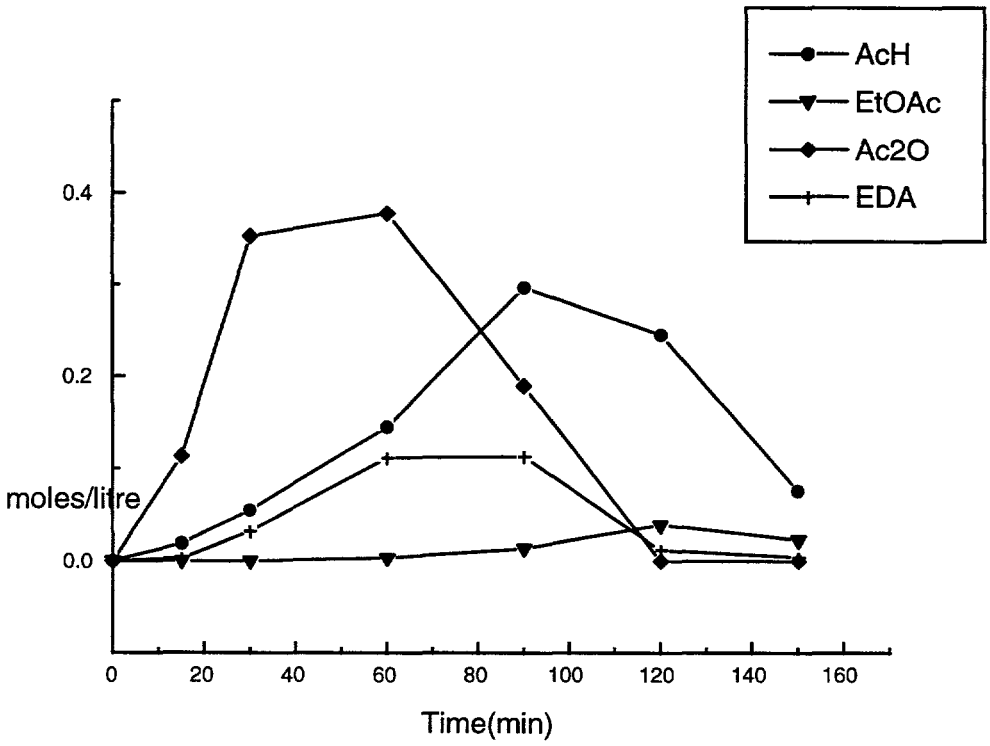

Figure 3.2.2 Reaction Profile Under Batch Mode

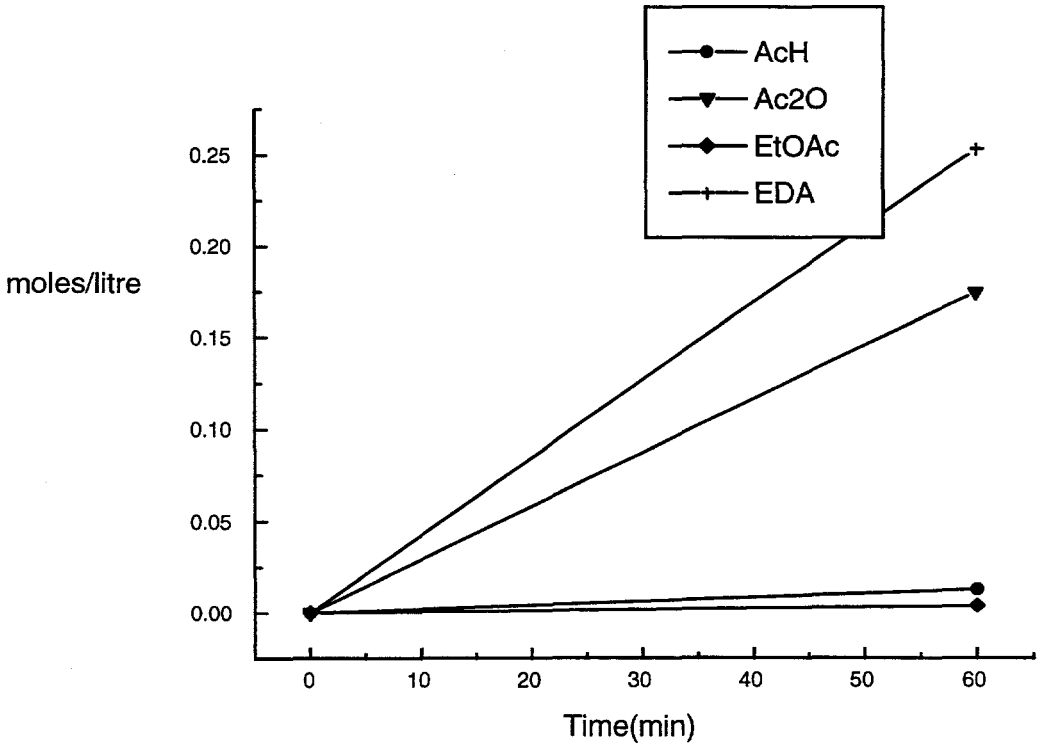

Heterogeneous Catalysis (Batch vs Sampling Mode)

The heterogeneous catalysts of interest were various Reillex polymers containing the ionically bound complex $[Rh(CO)_2I_2]^-$. The results of the experiments are summarized in Table 3.2.1. Also shown in this table are data from a sampling mode, Sample 1. All other data were obtained in a batch mode and include the suffix B in the sample number. The reaction conditions were similar to those described previously for the homogeneous reaction.

Table 3.2.1 Results of Heterogeneous Catalytic Runs

Sample Number	Time (min.)	Conv. (%)	MeOAc (%)	Ac2O (%)	AcH (%)	EDA (%)	EtOAc (%)	MB (%)
1.	60	100	35.3	30.4	10.5	12.4	2.2	90.8
2.	120	100	5.6	19.7	18.0	17.9	7.7	68.9
3B.	60	100	43.8	14.6	5.2	20.4	1.45	85.5
4B.	120	100	15.1	7.6	10.8	35.1	5.0	74.4
5B.	120	100	18.2	6.2	7.0	35.5	4.5	91*
6B.	60	100	44.7	10.3	3.8	22.1	1.8	93.3*
7B.	120	100	11.5	4.4	9.8	36.0	6.0	89.0*

* Mass Balance (MB) includes methane.
Note: 6B, 7B are REILLEX HP POLYMER; 2.24% Rh
3B, 4B are REILLEX 425 POLYMER; 2.24% Rh
5B is a REILLEX 425 POLYMER; 5.1% Rh

In Table 3.2.1 comparisons are made between the run labeled 3B and the run labeled 1 at the 60 minute mark. Both runs used Reillex 425 polymer containing 2.24% Rh by weight. In both of these runs the conversion of DME is close to 100%; however the batch run shows a higher EDA selectivity (20.4%) versus the sampling mode (12.4%). Also, the batch run shows a different selectivity order (EDA> Ac_2O> AcH) when compared to the sampling mode (Ac_2O> EDA> AcH). The batch run labeled 4B and run for 120 minutes shows an EDA selectivity of 35.1%, which is approximately twice that obtained for 2 at 120 minutes. Once again the product selectivity order EDA> AcH> Ac_2O for the batch mode is different from the sampling mode: Ac_2O> AcH = EDA. The samples labeled 6B and 7B were obtained by using a Reillex HP polymer containing 2.24% Rh by weight. Once again, Table 3.2.1 shows that the results obtained are almost identical to the batch reactions with the Reillex 425 polymer. Finally, a batch experiment with a Reillex 425 that contained ~ 5.1% Rh by weight was run. The overall weight of material used was adjusted so as to contain the same weight of Rh as the earlier runs

containing 2.24% Rh by weight. The objective here was to see if the distribution of Rh loaded on the polymer made a difference in the catalytic activity. A comparison of 5B versus 4B for 120 minutes shows almost identical results, demonstrating that it is the overall weight of rhodium that decides the activity.

Conclusions

The catalytic runs in a batch mode (homogeneous or heterogeneous) give better selectivity for EDA and a different selectivity order than the analogous reactions in a sampling mode. Future work will address understanding this effect.

Results and Discussion for Covalent Bound Catalyst

Experiments were conducted on a literature-reported heterogeneous catalyst (USP5371274) to convert MeOAc to EDA in the presence of syngas. The catalyst consisted of the complex $RhClCO(PPh_3)_2$ covalently linked to a phosphinated divinylbenzene polystyrene copolymer. With the described patent procedure, a polymer containing 1.8 wt % Rh was prepared and tested as a catalyst for the MeOAc conversion to EDA of a 1:1 CO/H_2 mix at 150°C and 1000 psi. The patent mentions the use of 3-picoline as an accelerator. The turnover number for EDA was calculated as moles of EDA/moles of Rh x time; a turnover number of 169 hr^{-1} was obtained. In contrast, the same reaction without the use of promoter gave a turnover number of 15 hr^{-1}.

The reaction was also studied with the ionically bound 5.1% Rh on Reillex using a comparable weight of polymer to have a weight of Rh identical to that in the covalently bound polymer. The results without promoter 3-picoline gave an EDA turnover of 14.6 hr^{-1}. In contrast, addition of 3-picoline improved the EDA turnover to 162 hr^{-1}. Therefore the results are similar to those obtained with the covalently bound polymer. We tried to improve the turnover number without the use of 3-picoline by adding an excess of Reillex polymer to the catalytic reaction. The objective was to provide promoter sites on the heterogeneous catalyst. Although there was some improvement in EDA turnover to ~ 20 hr^{-1}, the tremendous rate increase was not observed with 3-picoline.

Experiments were also conducted to recycle the Reillex catalyst in the presence of 3-picoline as the promoter. The yield of EDA in 4 hr decreased dramatically from 21% in the first run to 4% in the second to 0.5% in the third run, proving that 3-picoline is leaching Rh from our catalyst. The novelty of the Reillex catalyst for the DME to EDA conversion is that there is no need for any promoter and the catalyst can be recycled without loss in activity. The use of the Reillex polymer also allows operation at higher temperatures (190°C) compared to the gel-based polymer described in the patent.

(ii) Ethylidene Diacetate to Vinyl Acetate

Background

Ethylidene diacetate (EDA) $\{CH_3CH(O_2CCH_3)_2\}$ can be cracked to vinyl acetate (VAM) $\{CH_2 = CHO_2CCH_3\}$ and acetic acid (AcOH) $\{CH_3CO_2H\}$. Ethylidene diacetate (EDA) can also react to yield acetic anhydride (Ac_2O) $\{(CH_3CO)_2\}$ and acetaldehyde (AcH) $\{CH_3C(O)H\}$. Reaction 1 depicts this series.

$$Ac2O + AcH \longleftrightarrow EDA \longleftrightarrow VAM + AcOH \qquad \text{Rxn. 1}$$

In order to suppress the reaction to Ac_2O, previous work involved co-feeding Ac_2O. Previous cracking work also involved an acid catalyst such as p-TSA (para-Toluene Sulfonic Acid).

Gas Phase Cracking

Several catalysts, including an acidic carbon, a de-aluminized Y zeolite, and several coated carbons, were examined in a standard gas phase flow system. One gram samples of catalysts were loaded in a stainless steel reactor tube and brought to a temperature of 180°C in flowing nitrogen (10 cc/min). A feed of ethylidene diacetate, 0.2 ml/hr liq., was vaporized and introduced and the reaction products were monitored by gas chromatography. GC confirmed the presence of acetic anhydride, acetic acid, acetaldehyde, and unreacted ethylidene acetate. Based upon the acetic acid produced, the VAM production should have been substantial. The absence of vinyl acetate was unexplained.

Based on the quantity of acetic acid produced, the absence of VAM was disturbing. A series of temperature profile runs with VAM as a feedstock confirmed that vinyl acetate was thermally stable at temperatures up to 180°C in our reactor system. Further testing with a VAM feedstock and a catalyst in place confirmed that the catalyst was neither destroying nor adsorbing the VAM. The absence of acetylene in the product stream also indicated that the VAM was not being decomposed in another pathway.

In order to suppress the reverse reaction to acetic anhydride and acetaldehyde, the liquid feed was changed to a 50:50 mole % EDA/Ac_2O feed. Other parameters were maintained as they were previously. The product slate was essentially the same as seen above: Ac_2O, AcOH, AcH, and EDA. The presence of acetaldehyde indicated that EDA was still being reacted to Ac_2O and AcH, even though Ac_2O was a substantial component of the feed.

The most plausible explanation for this unexpected chemistry involves the probable hydroxyl sites present on the catalyst surface. If these sites react with Ac_2O, they yield acetic acid and leave acetate on the catalyst. In this reaction, the Ac_2O concentration is lowered, allowing EDA to react to produce more Ac_2O and AcH, thus explaining the presence of AcH and the absence of VAM. Reactions 2 and 3 diagram this.

$$Ac2O + HO^- \longrightarrow AcOH + AcO^- \qquad \text{Rxn2}$$

$$EDA \longrightarrow Ac2O + AcH \qquad \text{Rxn3}$$

Liquid Phase Cracking

Attempts were initiated to examine cracking of EDA in the liquid phase. A 15 gram sample of EDA was loaded into a 50 cc stirred reactor, and a 0.2 gram sample of ion-exchange resin (IER) was added. The reactor was sealed and heated to 150°C with stirring. After 4 hours, the reactor contents were transferred through a filter into an evacuated sample bomb. Subsequent analysis by manual injection showed that no reaction had taken place. At 150°C, with a known strong acid catalyst, no reaction occurs in a closed system. Based upon this, several conclusions can be drawn concerning the equilibrium of reaction 1.

Rxn.1

K1 must be large with respect to formation of EDA. K2 must be small and hence formation of VAM is unfavored.

Distillation Cracking

Based upon the equilibrium deductions above, in order to drive the reaction toward VAM and AcOH, one or both of the products must be removed as it is produced. A simple distillation with reflux was constructed. EDA and an IER (ion exchange resin) were loaded into a round bottom flask and brought to boiling. The distillate collected showed acetaldehyde, acetic anhydride, acetone, and vinyl acetate. Analysis of the pot showed DME (or a compound with the same retention time), acetic acid, acetic anhydride, and unreacted EDA. This product slate matches the predicted chemistry. More important, the presence of significant amounts of VAM is encouraging. Mass balances and conversions will be reported next quarterly.

An attempt to crack EDA thermally, without catalyst, led to simply distilling the EDA with no cracking. An attempt to base catalyze the reaction using MgO also led to no reaction.

Future work will examine a continuous distillation method to crack EDA to VAM while eliminating the reaction to Ac_2O. The goal is to reduce the cracking temperature to 100-110°C, which is within the thermal limits of an IER.

1Q FY96 Objectives

Future plans for Task 3.2 will focus on the following areas:

- Continue to screen immobilized catalyst candidates for hydrocarbonylation of dimethyl ether to ethylidene diacetate.
- Continue catalyst development work on the cracking of ethylidene diacetate to vinyl acetate and acetic acid.

Value Added Acetyls From Syngas (Eastman Chemical Company)

A. Introduction

The overall objective of this project is to produce a commercially viable process for the generation of vinyl acetate monomer (VAM) based entirely upon coal generated syngas (Scheme 1). Previous attempts at this objective have generally involved the combination of acetic anhydride (generated by carbonylation of either dimethyl ether or methyl acetate) with acetaldehyde (generated by either hydrogenation of acetic anhydride (Ac_2O) or hydrocarbonylation of either methanol (MeOH) or a methyl ester) to generate ethylidene diacetate (EDA), which is subsequently cracked to form VAM in a separate step. An exemplary process is shown below:

2 MeOH + 2 AcOH	→	2 AcOMe + 2 H_2O
AcOMe + CO + H_2	→	AcH + AcOH
AcOMe + CO	→	Ac_2O
Ac_2O + AcH	→	EDA
EDA	→	VAM + AcOH

AcH = acetaldehyde
AcOMe = methyl acetate

These efforts have failed to generate a commercially viable process to date. One of the key reasons for this failure was the very large quantities of recycled acetic acid (and consequently large commercial facilities) inherent in the earlier proposed processes.

Eastman's proposal was to circumvent the recycle problem by generating AcH by hydrogenation of acetic acid (AcOH) instead of by reductive carbonylation. Unfortunately, this process is thermodynamically disfavored and, even if acetic acid is hydrogenated, the conditions required generally favor further hydrogenation to form ethanol and ethyl acetate, which are the thermodynamically favored products. Currently, any processes that have successfully hydrogenated a carboxylic acid circumvent this problem by operating at unacceptably high pressures and temperatures to overcome the thermodynamic constrictions and by operating at low conversion to minimize over hydrogenation to the alcohol.

Eastman's proposed solution to this dilemma was to convert the acetic acid to ketene (a very well known process) and utilize the high energy content of the unstable ketene intermediate to overcome the thermodynamic constrictions to hydrogenation. The key task would be to identify catalysts that hydrogenated the ketene intermediate selectively to acetaldehyde (particularly did not generate ethanol or ethyl acetate) and would do so at commercially desirable temperatures and pressures.

Several restrictions are inherent in the contemplated conversion. Due to the unstable nature of ketene, the vapor pressure of ketene in the process should be less than atmospheric and its conversion should be reasonably high. Further, recovery of acetaldehyde will require that there not be excessive amounts of additional hydrogen present. Prior to this study, no catalyst was known for accomplishing this task.

Whereas the hydrogenation of acetic acid represented the linchpin technology in the proposal, the proposal also included some advances in the subsequent conversion of acetaldehyde to VAM. Obviously, the acetaldehyde thus formed could be converted to EDA and subsequently to VAM by known methods; Eastman proposed several improvements upon this known process. However, Eastman also proposed a very speculative application of ketene for the direct esterification of acetaldehyde to yield VAM without the intermediate generation of significant amounts of EDA. If this speculative conversion came to fruition, the overall process would be represented by the following relatively simple scheme: